COMBINING REGULARIZATION FRAMEWORKS FOR IMAGE DEBLURRING: OPTIMIZATION OF COMBINED HYPER-PARAMETERS

R. Youmaran and A. Adler

youmaran@site.uottawa.ca, adler@site.uottawa.ca,

School of Information Technology and Engineering (*SITE*)

University Of Ottawa

Abstract Regularization is an important tool for restoration of images from noisy and blurred data obtained from an ill-conditioned system. In this paper, we present a novel regularization technique (CGTik) that augments the conjugate gradient least-square (CGLS) algorithm with a Tikhonov-like prior information term. CGTik shows improved image reconstructions and increased robustness (in terms of sensitivity to data noise, and hyper-parameter choice) than CGLS or Tikhonov algorithms, with no increase in computational load compared to CGLS. This technique requires the appropriate selection of two hyper-parameters, the number of iterations (N) and amount of regularization (α). A method to select good values for these parameters is developed based on the L-curve technique for iterative methods where the 2^{nd} order gradient is used to select the L-curve with the largest rate of change and thus the most well defined corner. After the selection of α from the L-curve, N is chosen at point where the residual norm stops decreasing. Tests

were performed by calculating reconstructed images for each algorithm for heavily blurred and noisy images, and calculating the output image power spectral density (PSD). CGTik showed approximately three times reduction in high frequency noise compared to CGLS at the same number of iterations. CGTik showed visually improved restored images compared to Tikhonov and CGLS. Thus CGTik appears to offer a blend of the advantages of Tikhonov and CGLS image restoration.

Keywords: Image Restoration, Regularization, Tikhonov, inverse problems, iterative methods, ill-posed problems

1. INTRODUCTION

Image restoration and reconstruction are widely used techniques in applications where an unknown and desired image $f(x, y)$ must be recovered from a set of distorted data $g(x, y)$. In astronomy, for example, there is great interest in restoring images taken from satellites, which are frequently degraded by the effects of atmospheric turbulence and additive detection noise [29]. Another important application is restoring images degraded by motion blur introduced by a moving camera or target. These problems cannot be solved by simple filtering since they tend to be ill-posed such that small perturbations in the data introduce large fluctuations in the solution. If the system is linear and shift invariant, the relationship between the unknown and observed image can be described by a point-spread-function (PSF) distortion model $h(x, y)$ [13]. Unfortunately, blurring makes the restoration

problem ill-conditioned, and therefore not amenable to direct matrix inverse techniques, leading to noise amplification [3]. Regularization methods solve this problem by adding constraints to the formulation of the estimate.

The classic Tikhonov regularization technique [2, 3, 10, 18] estimates an approximate solution by augmenting the matrix formulation of the inverse with an image fidelity term based on some source of prior information. The most common Tikhonov formulations impose a smoothness constraint, and have the effect of low pass filtering the image estimate, thus blurring image edges. Tikhonov regularization requires the selection of a regularization parameter α that controls the tradeoff between fidelity to measurements and to prior information [4, 25, 27]. α controls the amount of smoothness introduced in the image estimate. It can be selected using the L-curve or the Generalized Cross-Validation (GCV) approach described in [25, 27]. If the Discrete Picard Condition described by *Hansen* in [28] is respected, it is preferable to use the L-curve approach since it makes use of both the residual and solution norms for the estimation of the hyper-parameter.

The Conjugate Gradient Least-square (CGLS) [5, 7, 27] is an iterative image reconstruction algorithm that can be viewed as a regularization method because the low frequency image components converge much faster than the high-frequency ones. The CGLS hyper-parameter is thus the number of iterations (N). Recently, iterative methods like CGLS have been extensively studied in the image reconstruction and restoration area particularly for image regularization on large images [13, 30]. The CGLS technique can be used to restore images with sharp discontinuities by using a higher N. If N is large a greater portion of the high frequency image content will converge, and, therefore, details are

recovered. However, noise amplification becomes a limitation of this technique since noise is amplified as N increases.

This paper proposes a new algorithm (CGTik) formulated as an iterative CGLS inverse augmented with a Tikhonov-like image prior information term. The CGLS algorithm is used to efficiently solve the least-square minimization representation of the Tikhonov formulation. Essentially, we wanted to explore the advantages of combining these different strategies, to see if an overall improved result could be obtained. We are aware that newer non-linear regularization schemes (such as total variation [27]) are able to improve on the performance of the linear regularization algorithms considered here. However, the disadvantage of such non-linear schemes is the large computational requirement, while CGTik is no more computationally intensive than CGLS. While techniques exist to choose an optimum value for single hyper-parameters, these techniques are not adequate for this algorithm, in which two hyper-parameters, α and N, are required. We develop an approach based on the L-curve technique to choose parameter values. First, α is selected based on the L-curve that presents the most appropriate L-shape and most well defined corner. Subsequently, N is selected at the corner of the curve with the best L-shape, as the point where the residual norm stops decreasing.

2. METHODS

We consider an image observation model described in matrix-vector form as:

$$\mathbf{g} = \mathbf{H}\mathbf{f} + \mathbf{n} \tag{1}$$

where $\mathbf{g}$ and $\mathbf{f}$ are lexicographically stacked image vectors of length *MN (width×height)* sampled on a 2-D rectangular lattice, and **H** is an *MN* x *MN* linear space-invariant operator that characterizes the image degradation. **n** is a vector of length *MN* of additive white Gaussian noise. The goal is to solve for an acceptable estimate $\hat{\mathbf{f}}$ of the original image.

2.1 Tikhonov Regularization

Tikhonov Regularization [18, 25] estimates an image $\hat{\mathbf{f}}_{\mathbf{tik}}$ such that:

$$\hat{\mathbf{f}}_{\mathbf{tik}}(\alpha) = \underset{\mathbf{f}}{\mathbf{argmin}} \left\| \mathbf{g} - \mathbf{H}\mathbf{f} \right\|_2^2 + \alpha \left\| \mathbf{L}\mathbf{f} \right\|_2^2 \tag{2}$$

where $\|.\|_2^2$ denotes the L-2 norm. The first term measures the fidelity of the solution to the data while the second term measures the fidelity to prior knowledge expressed in operator **L**. α represents the amount of regularization, and controls the tradeoff between these terms. If α is too large, the restored image will be blurred or over-regularized. On the other hand, if α is too small, noise will dominate the solution and it is said to be under-regularized. α is often selected using the L-curve technique [2,17,27]. The solution norm $\|f\|$ versus the residual norm $\|g - Hf\|$ is plotted on logarithmic axes for each value of the regularization parameter. The L-curve technique selects α at the point of maximum curvature. **L** is often chosen to be a smoothing function such as the identity matrix or the

Laplace operator $\mathbf{D}$. In this case, $\|\mathbf{Df}\|$ is a measure of roughness of the solution. The minimizer of (2) expressed as normal equations is:

$$(\mathbf{H}^T\mathbf{H}+\alpha\mathbf{L}^T\mathbf{L})\hat{\mathbf{f}}_{\mathbf{tik}}=\mathbf{H}^T\mathbf{g} \tag{3}$$

where $\mathbf{H}$ and $\mathbf{L}$ are block Toeplitz matrices. Equation (3) can be solved by singular value decomposition (SVD), factorization or by iteration [7, 9, 11, 13]. It can be seen in (3) how the regularization term $\alpha\mathbf{L}^T\mathbf{L}$ stabilizes the solution when the singular values of the system matrix $\mathbf{H}$ tend to be smaller as the rank of the matrix increases. If α is zero, the solution norm in (3) will be large since no regularization used. As α increases, the term $H^T g$ decreases and additional smoothing is introduced to the solution in order to suppress high frequency content and stabilize the estimate in the presence of noise.

2.2 The conjugate Gradient Least-Square Method (CGLS)

Another class of restoration techniques are iterative methods, which can be interpreted as regularization techniques in which the regularization parameter is the number of iterations. The Conjugate Gradient (CG) [5] technique solves positive definite equations of the form Ax = b. The conjugate gradient least-square method (CGLS) [6, 7, 10, 27] solves for $\hat{\mathbf{f}}_{\mathbf{cgls}}$ as:

$$\hat{\mathbf{f}}_{\mathbf{cgls}}=\arg\min_{\mathbf{f}}\|\mathbf{Hf}-\mathbf{g}\|_2^2 \tag{4}$$

by applying the Conjugate Gradient (CG) algorithm to the set of normal equations:

$$\mathbf{H}^{\mathrm{T}}\mathbf{H}\hat{\mathbf{f}}_{\mathbf{cgls}} = \mathbf{H}^{\mathrm{T}}\mathbf{g} \tag{5}$$

where the residual vector $\left\|\mathbf{H}\hat{\mathbf{f}}_{\mathbf{cgls}} - \mathbf{g}\right\|_2^2$ measuring the difference between the estimated solution and the original data vector is expressed as:

$$\begin{aligned}\mathbf{r} &= \mathbf{H}^{\mathrm{T}}\mathbf{H}\hat{\mathbf{f}}_{\mathbf{cgls}} - \mathbf{H}^{\mathrm{T}}\mathbf{g} \\ &= \mathbf{H}^{\mathrm{T}}(\mathbf{H}\hat{\mathbf{f}}_{\mathbf{cgls}} - \mathbf{g})\end{aligned} \tag{6}$$

$\hat{\mathbf{f}}_{\mathbf{cgls}}$ is calculated as described in [10]. Iterations are stopped (7) when the residual is less than a predefined tolerance δ:

$$\left\|\mathbf{H}\hat{\mathbf{f}}_{\mathbf{cgls}} - \mathbf{g}\right\|_2^2 < \delta \tag{7}$$

Note that expression (4) is equivalent to the Tikhonov equation (2) with no regularization term (i.e. α=0). The low-frequency components of the CGLS restored image tend to converge faster than the high-frequency components [5, 6]. Thus, in order to control high-frequency noise in the solution, *N* plays the role of regularization parameter.

2. 3 Proposed Method

The proposed iterative method (CGTik) uses the structure of the iterative Conjugate Gradient least-square minimization algorithm, and introduces a Tikhonov-like parameter to control the smoothing level in the regularized image. The difference between CGLS and CGTik is that the latter uses a regularization constraint to stabilize the solution. The CGTik estimate can be represented as follows:

$$\hat{\mathbf{f}}_{\mathbf{CGTik}}(\alpha) = \arg\min_{\mathbf{f}} \quad \left\| \mathbf{H}' \mathbf{f} - \mathbf{g}' \right\|_2^2$$

where (8)

$$\mathbf{H}' = \begin{bmatrix} \mathbf{H} \\ \alpha\mathbf{L} \end{bmatrix} \textbf{ and } \quad \mathbf{g}' = \begin{bmatrix} \mathbf{g} \\ \mathbf{0} \end{bmatrix}$$

This is equivalent to solving the Tikhonov least-square problem formulated as follows:

$$\begin{aligned} \hat{f}_{Tik}(\alpha) &= \arg\min_{f} \quad \left\| \begin{matrix} Hf - g \\ \alpha Lf \end{matrix} \right\|_2^2 \\ &= \arg\min_{f} \left[\sum_{i=1}^{MxN} (Hf - g)_i^2 + \sum_{i=1}^{MxN} (\alpha Lf)_i^2 \right] \\ &= \arg\min_{f} \left\| g - Hf \right\|_2^2 + \alpha \left\| Lf \right\|_2^2 \end{aligned}$$

Equation (8) is then solved by CGLS [7, 10] with the augmented terms *H'* and *g'*. This differs from Tikhonov regularization since the algorithm is stopped before the singular vectors completely converge. For this solution, two parameters, *N* and α must be appropriately selected. The regularizer "α**L**" incorporated into the CGLS least-square formulation will penalize non-smooth components in the estimate and control noise amplification. Thus, CGTik introduces additional smoothing which slows the convergence of high frequency components.

2.3.1 Regularization Parameter selection. Appropriate selection of the regularization parameters is important to achieve good restoration. If α is too small, noise will dominate the solution; if it is too large, the resulting image will be over blurred. As mentioned previously, for Tikhonov-like regularization, α may be selected using the L-curve

technique ([2]). In order to select appropriate regularization parameters for CGTik, we propose a framework based on the L-curve technique for an iterative method. In this case, each L-curve represents one value of α, which is repeated for multiple parameters, as illustrated in Fig. 1:

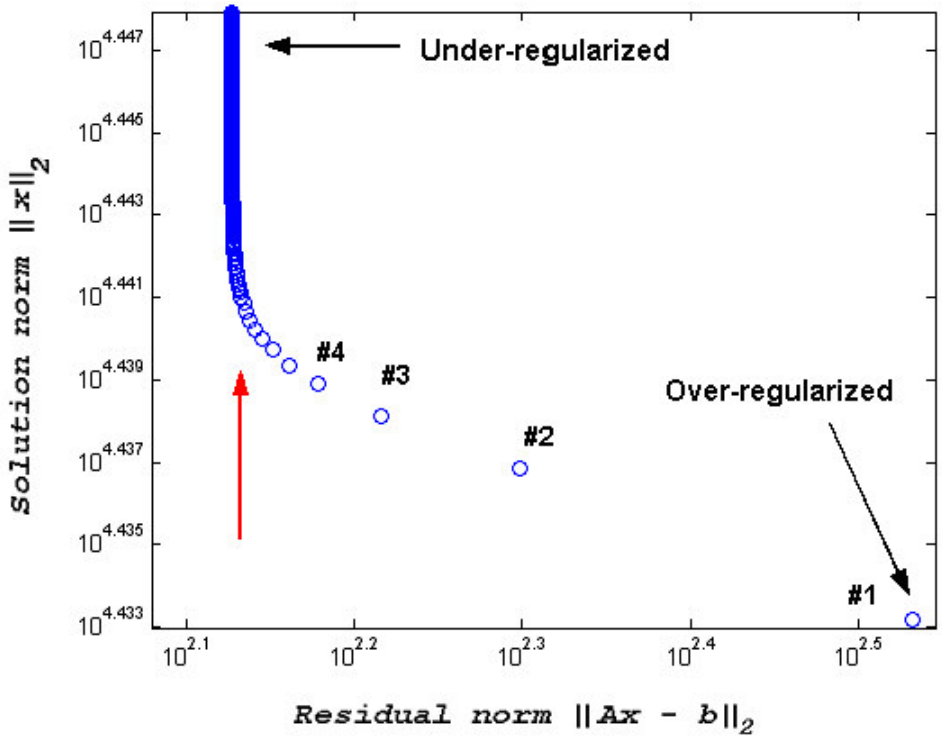

Figure 1: ***L-curve for a typical CGLS solution: Solution norm versus Residual norm for one regularization parameter value and N=200 iterations. The curve typically displays a knee-shaped structure, and the optimal regularization parameter is at the point of maximum curvature, indicated by the arrow.***

In Fig. 1, the first iteration of image restoration (indicated by point #1) is a blurred image located in the over-regularized region at the lower right hand side where the data is not well fitted but the solution norm is very small. As the number of iterations increases, the residual norm decreases with little change in solution norm until the optimal number of iterations is reached at the corner of the curve. Afterwards, the solution norm increases rapidly while the data norm remains essentially unchanged. This indicates the noise

amplification process, which is avoided by stopping the algorithm. In order to apply the L-curve for CGTik, it is necessary to start by approximating a range of α values where the image estimates are acceptable. Subsequently, CGTik is run for *N* iterations for a range of values of α, and the corresponding L-curves are calculated. The following diagram illustrates the method for parameter selection:

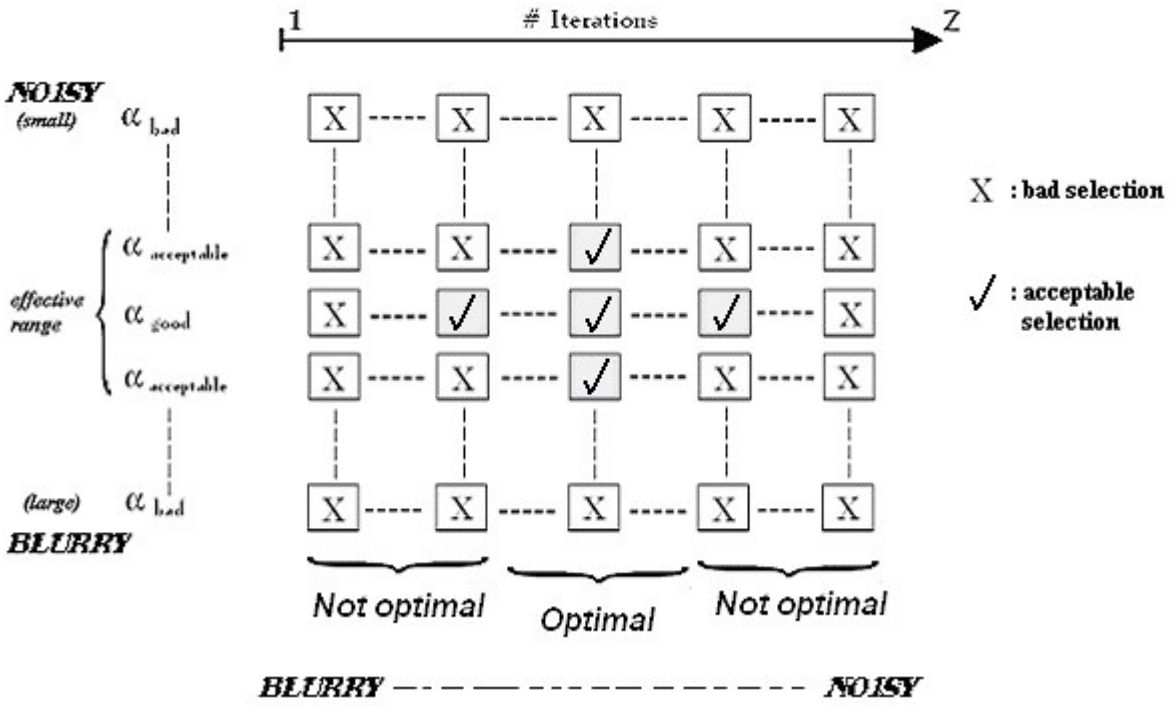

Figure 2: Block diagram illustrating the proposed approach for selecting α and N parameters in CGTik

An ideal hyper-parameter corresponds to a solution in the middle region of the block diagram in Fig. 2. α and *N* are chosen at the point with the most well defined "knee-shape" edge on the L-curve plot with the steepest descent. For example, if α is too small and *N* is too large, the algorithm converges to under-regularized solutions and remains in the upper right quadrant of the diagram.

2.3.2 *Automated Regularization Parameter selection*

In order to allow for automatic selection of hyper-parameters for CGTik, we have developed the following method based on the L-curve technique [10], as follows:

1) Choose an arbitrary range of α values that includes the optimal solution. The effective α values are the ones that provide acceptable L-curves and plausible solutions.
2) Using CGTik, compute all L-curves that correspond to the effective α values (Fig. 3) selected for our specific problem and plot them for a fixed N_{max}, chosen to be large in order to ensure convergence of all high-frequencies in the restored image.
3) Interpolate (using linear interpolation) the L-curves onto N_{max} sample points evenly spaced in log residual value in order to ensure that enough data points are allocated to the first few iterations on the curve where the residual norm decreases rapidly. This will give discrete L-curves defined by N_{max} equally spaced sample points.
4) Normalize L-curves and calculate the 2^{nd} order gradient with respect to log residual value
5) Find N on the logarithmic (non-interpolated) L-curve as the point where the residual norm stops decreasing as shown in equation 7, where δ is set to a value very close to zero.

6) If the N computed in step 5 is equal to the N_{max} selected by the algorithm, then the value selected for N_{max} is too small. Restart the entire procedure with a larger value of N_{max}.

The reasoning behind this algorithm is to detect the curvature in the L-curve where the highest 2nd order gradient represents the curve with the steepest slope in the vertical direction and the most well defined corner. If two curves have identical slopes in the vertical direction but differing tilt in the horizontal direction, the one with the smallest tilt is selected representing a sharper transition from vertical (solution norm) to horizontal (residual norm) axis. Once the regularization parameter α is chosen, N is selected on the candidate curve as the sample point where the residual norm stops decreasing and the solution norm increases rapidly. This point is located at the corner of the ideal L-curve.

2.3.3 Test methodology. Results are shown using the "cameraman" image (170x170 pixels). Gaussian blur was applied and Gaussian white noise added (SNR=30 dB). The blur matrix H is an *MN x MN* symmetric, doubly block Toeplitz matrix (band=3) that models blurring of an image by a Gaussian point spread function of width σ=1 pixel. The original and blurred images are shown in Fig. 5 and 6 respectively. This image was then restored using the Tikhonov, CGLS, and the CGTik algorithms. The constraint L=D was used for the Tikhonov and CGTik algorithms. This constraint penalizes non-smooth content in the regularized image. For the CGTik method, a range of α values was selected and the L-curve plotted for each of them. The regularization results obtained are compared using the

noise power spectral density (PSD). To quantify the performance of the algorithms, the power spectral density (PSD) and improvement signal to noise ratio (ISNR) [11] are used. The PSD measures the image noise power as a function of frequency; restored images tend to have reduced high frequency noise compared to the original blurred noisy data. The ISNR is defined as:

$$\mathbf{ISNR} = 10\log\left[\frac{\|\mathbf{g}-\mathbf{f}\|_2^2}{\|\hat{\mathbf{f}}-\mathbf{f}\|_2^2}\right] \tag{9}$$

3. RESULTS

The restoration results of the degraded image in Fig. 6 are shown using Tikhonov (Fig. 7), CGLS (Fig. 8) and CGTik (Fig. 9). For Tikhonov solution, α=0.2 was chosen using the L-curve method. For the CGLS restoration, N=11 was chosen at which the restoration presented the best-perceived quality image. For the CGTik restoration, α and N were selected based on the L-curve with the ideal L-shape and the most well-defined corner (section 2.3.2), as shown below. Results show a significant improvement in perceived quality and a reduction of noise in the restored images, with CGTik showing a good compromise between the blur of the Tikhonov restoration, and the speckle-like noise of CGLS.

Fig. 3 illustrates the L-curves obtained by CGTik for the effective range of α values. As mentioned previously, in order to select an appropriate hyper-parameter using the L-curve method, the curve must have a well defined "knee-shaped" edge. This is illustrated by L-curves # [5,6,7,8,9] in Fig. 3. They correspond to the optimal parameters for this case.

Images were calculated using Matlab on a Pentium 4, 2.8GHz computer with 512 MB of Ram. 374 sec. were required for the image restoration process and ideal parameters selection using an effective range of 12 α values with *N*=200.

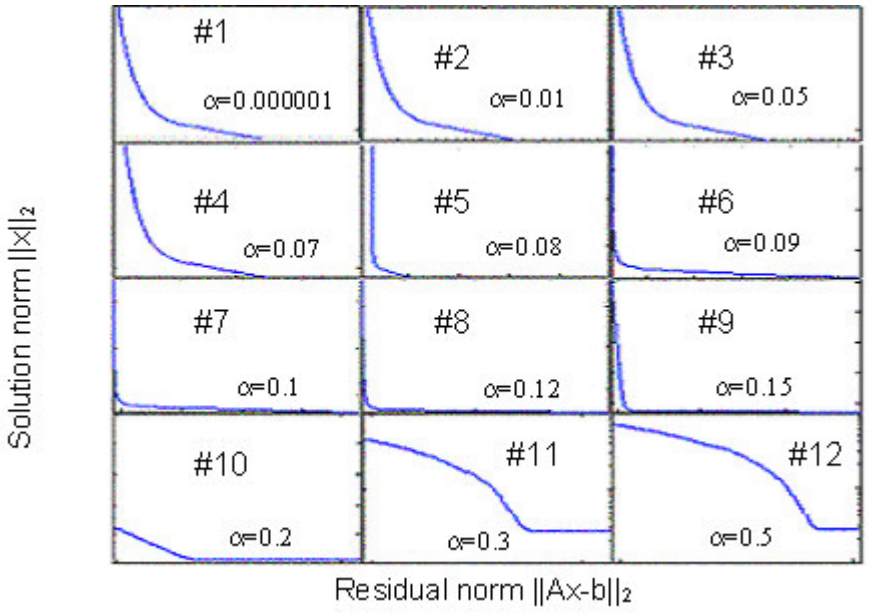

Figure 3: L-curve values for twelve different selections of α and N=200. Each sub-figure is a log-log plot of residual norm vs. solution norm. Axes are arbitrary but identical for each sub-figure. The ideal curves (5, 6, 7, 8, 9) have a well defined L-shape, a "knee-shaped" corner, and a steep slope (negative) representing the solution norm.

Once the L-curves are computed, the 2nd order gradient is calculated for each of them in order to approximate the ideal α. Based on this approach, L-curve #8 (α=0.12) presented

the highest 2nd order gradient since it has the steepest rate of change in the vertical direction and the smallest tilt in the horizontal direction as shown in Fig. 4.

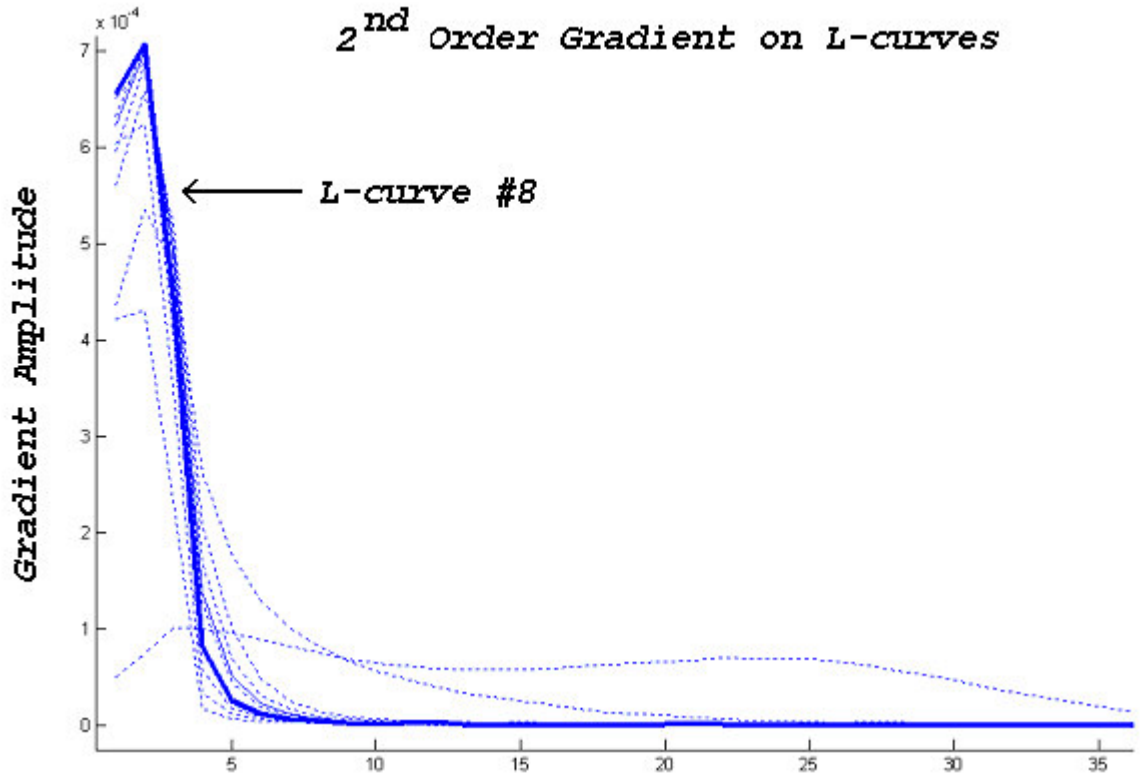

Figure 4: 2nd Order Gradient versus interpolated solution norm of 12 the L-curves of figure 3. The line (in bold) represents the highest 2nd order gradient and corresponds to L-curve #8 (α=0.12)

After the best L-curve is identified, *N* is computed based on the residual norm as the sample point where the residual stops decreasing. This is located at the corner of the ideal L-curve [#8] in Fig. 3 and corresponds to *N*=11 iterations.

Figure 5:Original image (170x170 pixels)

Figure 6: image with Gaussian blur and noise (SNR= 30 dB)

Figure 7: Tikhonov restoration (α=0.2)

Figure 8: CGLS restoration (N=8)

Figure 9: CGTik restoration (α=0.12 and N=11)

Figure 10: CGTik restoration using a large α (α=0.9)

The Tikhonov restoration in Fig. 7 shows an enhanced image where noise is removed and details are well recovered. The drawback is that when the method is tuned to completely suppress additive noise, it introduces edge blurring in the solution and the estimate tends to look blurry. There is a tradeoff between noise removal and edge blurring, controlled by α. On the other hand, iterative CGLS reduces the amount of blur in the restored image shown in Fig. 8 but amplifies high frequencies and introduces edge artefacts as N increases. In general, CGLS restorations tend to look noisier than Tikhonov but achieve better detail enhancement and blur reduction. The CGTik regularized image (Fig. 9), contains less high-frequency noise than the CGLS restoration (Fig. 8), and does not show the edge artefacts or ringing of the CGLS image (Fig. 8). CGTik reduces noise while removing blur since lower frequencies converge much faster than higher frequencies in the image. As α increases, additional smoothing is introduced to accelerate noise reduction and improve the quality of the image. The solution power spectrum density (PSD) (Fig. 11) shows that CGTik reduces high-frequency noise compared to CGLS with no impact on low-frequency

image components. This is due to the α factor in CGTik that attenuates noise while preserving most of the details in the image. If a large value is chosen for α, CGTik will produce unusable (over-regularized) solutions (Fig. 10, α=0.9).

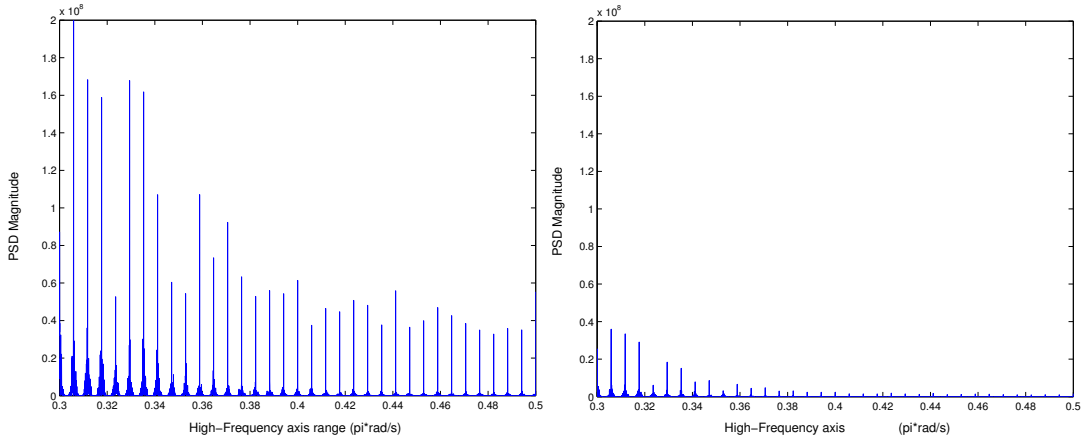

Figure 11: PSD plot for CGLS (left) and CGTik (right) showing superior noise attenuation by CGTik compared to CGLS restoration for the same frequency range (*N*=11 both cases).

The ISNR plot (Fig. 12) illustrates that CGTik provides better estimates with low noise level for a larger set of images and bigger number of iterations. Therefore, it is easier to select a good approximation using CGTik since the ISNR curve decreases less rapidly than CGLS curve.

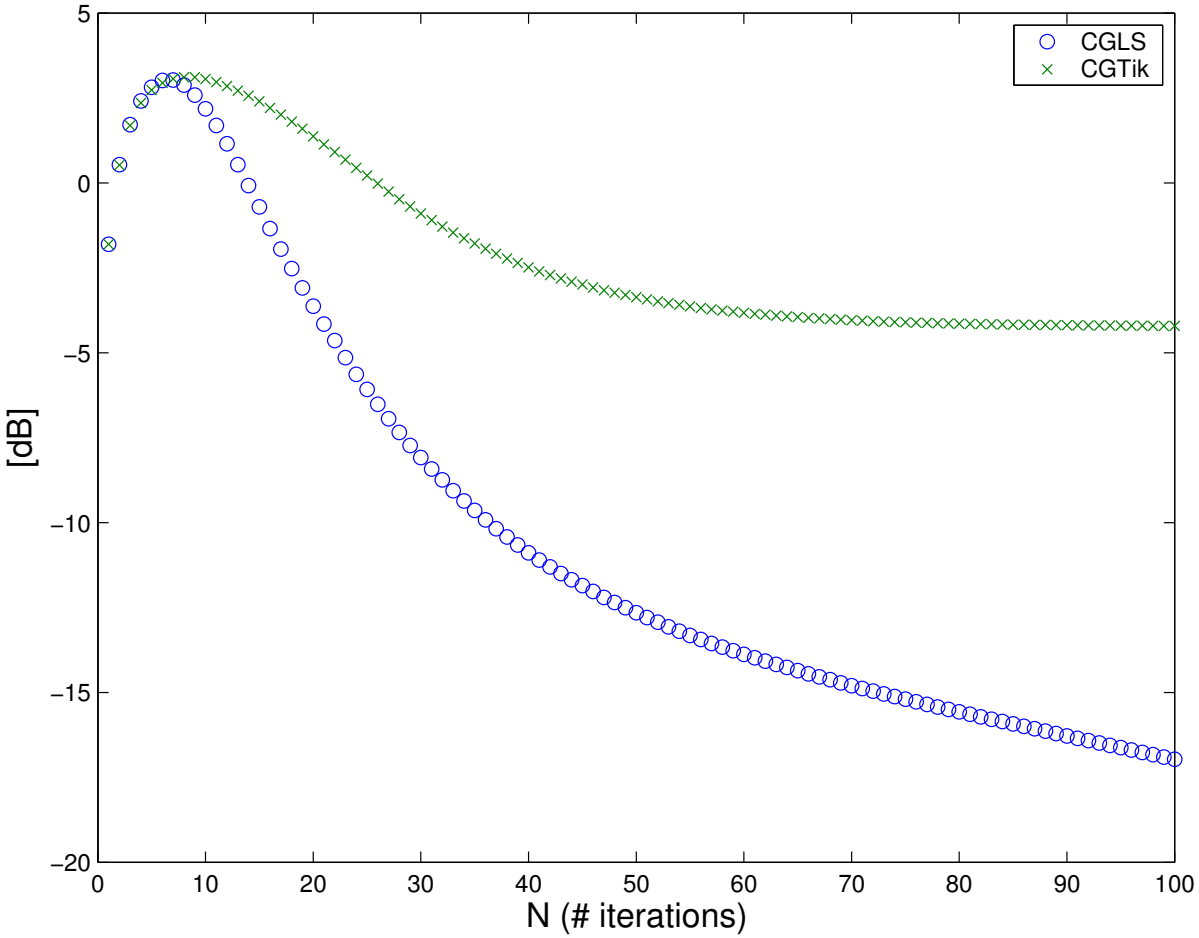

Figure 12: ISNR curves for CGLS and CGTik iterative methods

4. DISCUSSION AND CONCLUSION

This paper presents a novel regularization approach (CGTik) which combines Tikhonov and CGLS restoration techniques. Tikhonov regularization solves an ill-conditioned problem by the incorporation of prior information about the original image through the inclusion of an additional L-2 norm term to the least-square cost function. Typically, L=D

is chosen as a regularizer; it measures the image slope and favors solutions with limited high-frequency energy. Since quadratic L-2 based functions are used for the data and regularization terms in the Tikhonov formulation, this leads to a linear inverse filtering problem. One disadvantage of Tikhonov is that it reduces high-frequency energy causing edge blurring. Thus, Tikhonov is not well suited for solutions containing sharp discontinuities. CGLS solves the least-square cost function by minimizing the residual norm. For an ideal number of iterations (*N)*, the amount of blur can be reduced considerably in the restored image while keeping the noise level low. By combining CGLS and Tikhonov, the proposed approach performs better than either method at reducing blur and noise in the solution. Reconstructed images with CGTik showed better perceived quality, reduction of ringing artefacts, and noise attenuation in the PSD plot compared to CGLS.

An additional complication of CGTik is the requirement to select appropriate values of two hyper-parameters, α and *N*. An L-curve based technique is developed to select these parameters. First, α is chosen by the L-curve with the steepest vertical edge and the smallest tilt in the horizontal direction. *N* is subsequently selected at the point where the residual norm stops decreasing, corresponding to the corner of the L-curve. A disadvantage of CGTik is that its parameter choice is more computationally expensive, as these operations must be repeated for several candidate solutions. CGTik parameter selection process is approximately ten times longer than CGLS but the reconstruction procedure similar, being linear and thus fairly cheap.

CGTik has several advantages: 1) the restored images are visually better since blur is considerably reduced; 2) it shows greater noise reduction in the images compared to CGLS; 3) it provides a larger range of good solutions than CGLS. This is due to the introduction of the α parameter that controls the noise amplification process in the restored images as N increases; and 4) CGTik restorations have a larger ISNR for the same N, compared to CGLS. The CGTik algorithm can be tuned for more flexibility depending on the application and the characteristics of the degraded image. For example, when the image is smooth with few edges, α can be large since there is less concerns about edge blurring leading to a significant noise reduction. If the image contains contours and edges, α can be set to a small value to avoid additional blurring and while using a large N in order to recover the most detail in the estimate. In general, CGTik performs better on smooth images since it introduces some edge blurring in the solution. For applications where edge preservation is important, non-linear regularization techniques such as Total Variation [27] are probably more appropriate. On the other hand, non-linear regularization techniques are computationally expensive, whereas CGTik reconstruction benefits from the linear restoration. Additionally, it may be possible to modify equation 8 to account for the non-linear cost function norm. For example, the norm could be set to a lower value (such as 1.2) to allow a certain amount of edge preservation [31].

In conclusion, we have proposed a linear image restoration algorithm, CGTik, which combines the features of the Tikhonov and CGLS approaches. It demonstrates increased

robustness, and achieves improved image reconstructions than either of the source approaches, while maintaining a similar level of required computational power.

References

[1] P.C. Hansen, “Truncated singular value decomposition solutions to discrete ill-posed problems with ill-determined numerical rank”, SIAM J. Sci. Stat. Comput., vol.11, pp. 503-518, 1990

[2] P.C. Hansen and D.P. O’Leary, “The use of the L-curve in the regularization of discrete ill-posed problems”, *SIAM* J. Sci. Comput., vol. 14, pp.1487-1503, 1993.

[3] A. Neumaier, “Solving ill-conditioned and singular linear systems: a tutorial on regularization”, *SIAM* Review, 40(3), pp. 636-666, 1998.

[4] A.M. Thompson, J. C. Brown, J W. Kay and D.M. Titterington, “A study of methods of choosing the smoothing parameter in image restoration by regularization”, *IEEE* tran. PAMI, vol. 13, No.4, pp. 326-339, April 1991.

[5] T. Steihaug, “The conjugate gradient method and trust regions in large scale optimization”, *SIAM* J. Numer. Anal., 20(3), pp. 262-637, 1983.

[6] M.Hanke and P.C. Hansen, “Regularization methods for large-scale problems”, *Surveys Math*., pp. 253-315, 1994.

[7] P.C. Hansen, “Regularization Tools: a MATLAB package for analysis and solution of discrete ill-posed problems”, *Numer*. Algo., pp. 1-35, 1994.

[8] W. Zhu, Y. Wang, J. Chang, H. L. Graber, and R. L. Barbour, “A total least squares approach for the solution of the perturbation equation”, Proc. SPIE Conference on Optical Tomography, Photon Migration, and Spectroscopy of Tissue and Model Media, (San Jose, CA), Feb. 1995, vol. SPIE-2389, pp. 420-430.

[9] S. Van Huffel and J. Vandewalle, “The Total Least Squares Problem: Computational Aspects and Analysis”, *SIAM* Press, Philadelphia, 1991.

[10] Rick Aster, Brian Borchers, and Cliff Thurber, “Parameter Estimation and Inverse Problems”, *in preparation,* 2003.

[11] R.L. Lagendijk and J. Biemond, “Iterative Identification and Restoration of Images”, Norwell, MA: Kluwer Academic Publishers, 1991.

[12] Per Christian Hansen, “Rank–Deficient and Discrete Ill-Posed Problems: numerical aspects of linear inversion”, SIAM, Philadelphia, 1998.

[13] Jan Biemond, Reginald Lagendijk, Russell M. Mersereau, “Iterative Methods for Image Deblurring”, Proceedings of the IEEE, Volume: 78, pp.856 - 883, May 1990.

[14] Nicolaos B. Karayiannis, Anastasios N. Venetsanopoulos, “Regularization Theory in Image Restoration: The Stabilizing Functional Approach”, IEEE Transactions on Acoustics, Speech, and Signal Processing, 38(7), pp. 1155-1179, July 1990.

[15] Nikolas P. Galatsanos, Aggelos Katsaggelos, “Methods for Choosing the Regularization Parameter and Estimating the Noise Variance in Image Restoration and Their Relation”, Image Processing, IEEE Transactions, vol. 1, Issue: 3, pp. 322 – 336, July 1992.

[16] M.G. Kang, A.K. Katsaggelos, “Simultaneous Iterative Image Restoration and Evaluation of the Regularization Parameter”, Signal Processing, IEEE Transactions on [see also Acoustics, Speech, and Signal Processing], vol. 40, Issue: 9, pp. 2329 – 2334, Sept. 1992.

[17] C.M. Leung, W.-S. Lu, “An L-curve Approach to Optimal Determination of Regularization Parameter in Image Restoration”, Canadian Conference on Electrical and Computer Engineering, 14-17, vol.2, pp. 1021 – 1024, Sept. 1993.

[18] Irina F. Gorodnitsky, Bhaskar D. Rao, “ Analysis of Error Produced by Truncated SVD and Tikhonov Regularization Methods”, Twenty Eighth Asilomar Conference on Signals, Systems and Computers, Pacific Grove, CA, Oct. 31 - Nov. 2, 1994.

[19] C.M. Leung, W.-S. Lu, “Optimal Determination of Regularization Parameters and the Stabilizing Operator”, Communications, Computers, and Signal Processing Proceedings, IEEE Pacific Rim Conference on, pp. 403 – 406, May 1995.

[20] P. Lobel, Ch. Pichot, L. Blanc-Féraud, M. Barlaud, “Conjugate Gradient Algorithm with Edge-Preserving Regularization for Image Reconstruction from Experimental Data”, Antennas and Propagation Society International Symposium, AP-S Digest, vol. 1, 21-26 July 1996, pp. 644 – 647.

[21] Irina F. Gorodnitsky, Bhaskar D. Rao, “Truncated Total Least Squares Regularization Algorithm for Underdetermined Problems”, 7th SP Workshop on Statistical Sig. and Array Processing, June 1994.

[22] Wenwu Zhu, Yao Wang, Nikolas P. Galatsanos, Jun Zhang, “Regularized Total Least Squares Approach for Nonconvolutional Linear Inverse Problems”, Image Processing, IEEE Transactions on, vol. 8, Issue: 11, pp. 1657 – 1661, Nov. 1999.

[23] Wufan Chen, Ming Chen, Jie Zhou, “Adaptively Regularized Constraint Total Least-Squares Image Restoration”, Image Processing, IEEE Transactions on, Volume: 9, Issue: 4, pp. 588 – 596, April 2000.

[24] Luc Knockaert, Daniel De Zutter, “Regularization of the Moment Matrix Solution by a Nonquadratic Conjugate Gradient Method”, IEEE Transactions on Antennas and Propagation, vol. 48, Issue: 5, pp. 812 - 816, May 2000.

[25] Peter R. Johnston, Ramesh M. Gulrajani, “Selecting the Corner in the L-curve Approach to Tikhonov Regularization”, IEEE Transactions on Biomedical Engineering, vol. 47, Issue: 9, pp. 1293 - 1296, Sept.2000.

[26] Soontorn Oraintara, William C. Karl, David A. Castanon, Truong Q. Nguyen, “A Method for Choosing the Regularization Parameter in Generalized Tikhonov Regularized Linear Inverse Problems”, Image Processing Proceedings. 2000, International Conference on, vol. 1, pp. 93 – 96, Sept. 2000.

[27] Al Bovik (ed.), *Handbook of Image & Video Processing*, Academic Press, 2000 ISBN 0-12-119790-5.

[28] P.C. Hansen, “The Discrete Picard Condition for discrete ill-posed problems”, BIT, 30:658-672, 1990.

[29] Shi, X. and Ward, R.K., “Restoration of Images Degraded by Atmospheric Turbulence and Detection Noise,” Jour. of the Optical Society of America, A, Vol. 9, No. 3, March 1992, pp. 364-370.

[30] S. R. Arridge and M. Schweiger, “A general framework for iterative reconstruction algorithms in optical tomography, using a nite element method,” in Computational Radiology and Imaging: Therapy and Diagnosis C. Borgers and F. Natterer, eds., IMA Volumes in Mathematics and its Applications, 1998.

[31] Bouman C, Sauer K, “A generalized Gaussian image model for edge-preserving MAP estimation”, [Journal Paper] IEEE Transactions of Image Processing, vol.2, no.3, pp.296-310, July1993.